Journal of Engg. Research **Vol. 5 No. (6) March 2018 pp.** *1-14*

انقطاع وتحليل القدرة لشبكة الراديو المعرفية تحت تأثير التداخل الكلي عبر خبو ناكاغامي–m

فابهاف هندري*، ك.في. كارتيكيان، م. مورغان*** و م. م. ديشموخ*****

* باحث علمي في قسم هندسة الالكترونيات، جامعة ساثيباما، تشيناي، تاميل نادو، الهند

** قسم الإلكترونيات وهندسة الاتصالات، جامعة ساثيباما، تشيناي، تاميل نادو، الهند

*** قسم هندسة الالكترونيات والاتصالات، كلية الهندسة فالياماي، تشيناي، الهند

**** قسم هندسة الالكترونيات والاتصالات، كلية ترينيتي للهندسة والبحوث، بيون، مهاراشترا، الهند

* مراسلة المؤلفين بالبريد الإلكتروني: hendrevaibhav@gmail.com

الخـلاصـة

في شبكة إذاعية إدراكية، يعتمد أداء المستعملين الثانويين على التداخل في نفس القناة الذي تولده المرسلات الأولية والثانوية. ولذلك فإن توصيف التداخل الكلي في هذا النوع من الشبكات له أهمية قصوى. وقد تم الإبلاغ عن توصيف الذكاء الاصطناعي في المستقبل الأولي بسبب تعدد المستخدمين المعرفين في الأدب ولكن لم يتم التحقيق في تأثير هذا الذكاء الاصطناعي على أداء المستقبلات الثانوية.

في هذه الورقة، تم استنباط معادلات مقفلة لاحتمال الانقطاع استنادا إلى دالة التوزيع التراكمي للإشارة المستقبلة إلى النسبة في المرحلة الثانوية. وقد أجري هذا التحليل تحت تأثير الذكاء الاصطناعي الناجم عن العديد من الشبكات الثانوية تحت قناة الخبو–م ناكاغامي. تم تصميم النظام النموذجي على أساس أدوات الهندسة العشوائية حيث يفترض أن توزع العقد المسببة للتداخل بطريقة بواسون المتجانسة. علاوة على ذلك، تم استنباط معادلات مقفلة لتقدير قدرة الشبكات الثانوية لمتغيرات مختلفة لقناة ناكاجامي. وتبين النتائج ان احتمالات التخارج وإرغوديك القدرات لا تعتمد فقط على مستوى المستقبلات، بل أيضا على وظيفة الاستقبال التي يتلقاها المستقبل، وطوبولوجية الشبكة، ومتغيرات قنوات الخبو ناكاغامي.

Outage and ergodic capacity analysis for cognitive radio network under the impact of aggregate interference over Nakagami-m fading

Vaibhav Hendre*, K. V. Karthikeyan**, M. Murugan***, M. M. Deshmukh****

Department of Electronics & Telecommunication, G. H. Raisoni College of Engineering & Management, Pune

***Department of Electronics and Communication Engineering, Sathyabama University, Chennai, Tamilnadu, India*

****Electronics and Communication Engineering Department, SRM Valliammai Engineering College, Chennai, India*

*****Electronics and Telecommunication Engineering Department, Trinity College of Engineering & Research, Pune, Maharashtra, India*

**Correspondent Author: hendrevaibhav@gmail.com*

ABSTRACT

In a cognitive radio network (CRN), the performance of secondary users depends on the co-channel interference generated by the primary and the secondary transmitters. Therefore, the characterization of aggregate interference (AI) in such type of networks is of prime importance. The characterization of AI at the primary receiver due to multiple cognitive users has been reported in the literature, but the impact of this AI on the performance of secondary receivers has not been investigated. In this paper, the closed form expressions have been derived for the outage probability based on the complementary cumulative distribution function (CCDF) of the received signal to interference ratio (SIR) at secondary receiver. This analysis is carried out under the impact of AI generated by multiple secondary networks under Nakagami-m fading channel. The system model is designed based on stochastic geometry tools where the interfering nodes are assumed to be distributed as a homogeneous spatial Poisson point process (PPP). Further, the closed form expressions have been derived for the ergodic capacity of secondary networks for different parameters of the Nakagami-m fading channel. The results show that the outage probability and ergodic capacity depend upon not only the threshold level of the primary receivers but also a function of received SIR at the secondary receiver, network topology, and the parameters of Nakagami-m fading channels.

Keywords: Aggregate interference; cognitve radionetwork; ergodic capacity; Nakagami-m fading; outage probability.

INTRODUCTION

Cognitive radio network (CRN) has been researched over the last decade as an enabler of efficient spectrum utilization, in answer to the ever-increasing number of unlicensed wireless devices and applications in *Mitola &* (1999). One key aspect of deploying CRN is to never interfere with the operation of the licensed users, also referred to as primary users (PUs). There are three network paradigms proposed in the CRN: underlay, overlay, and interweave as in *Goldsmith & Mari* (2013). In the underlay mode, the power of SUs is kept very low so that it operates below the interference temperature of PUs. Only short distance secondary communications are possible by using the underlay mode in *Ahmad et al*. (2015). In the overlay mode, the PUs shares some information about the codebook with SUs. SUs help PUs avoid the interference created at the primary receiver with the help of this information. SUs also utilize this information to reduce the interference at the secondary receiver. Here, SUs also need to operate at very low powers. In the interweave mode, the SUs sense the unoccupied spectrum called spectrum hole of PUs. In coordination with PUs, the spectrum holes are utilized for data transmission by SUs as given in *Weifeng et al*. (2012).The interference averaging based underlay CRN allows the SUs to utilize the spectrum at the same time along with the PUs but under the strict constraints on the interference that happened to the PUs. Therefore, the characterization of aggregate interference (AI) at the PUs that happened due to multiple SUs is highly important in such networks.

On the other hand, the characterization of the AI at the SUs side is also critical to carry out the outage and capacity analysis of the secondary link. The characterization of the AI at any arbitrary point depends on the network topology, operational behavior, and the type of channel fading. The network topology describes the distribution of the secondary nodes in the network along with the primary ones. The operational behavior is based on an access mechanism, a power control mechanism, and a sensing mechanism. The outage-capacity analysis of the secondary link is also based on the type of channel fading. The concept of stochastic geometry was presented in *Baccelli & Blaszczyszyn* (2009) and *Haenggi et al*. (2009) to model the large wireless network where the nodes were assumed to be distributed spatially as a Poisson point process (PPP). The process of the interference characterization in a spatial PPP was discussed in *Haenggi et al*. (2009).

The impact of the transmit power and the carrier sense threshold on the network capacity was studied in *Yang et al*. (2007) for the scenario of multi-hop wireless networks. The characterization of the AI was done in *Jabbari & Babaei* (2008) based on the PPP by integrating over the area occupied by the non-sensing nodes. The power control mechanism was based on the maximum AI, but finally it was not estimated exactly in that work. The characterization of the AI for the CRN based on the power control, the contention control, and the hybrid control was studied in *Chen et al*. (2012). The outage capacity of the primary system was derived based on the PDF of the aggregate interference.

A CRN based on the IEEE 802.11 standard was considered in *Timmers et al*. (2012) to model the accumulative interference generated from a large-scale CRN. The impacts of the discrete topology of the SUs were considered in order to meet the interference constraints at PUs. *Haenggi & Ganti* (2009) presented the detailed analysis of the interference characterization and outage in regular multi-dimensional networks and Poisson networks. Closed form analytical expressions for

the moment generating function of the interference were derived in *Srinivasa & Haenggi* (2007) to evaluate the network outage performance. It was assumed that the finite and fixed numbers of nodes are distributed uniformly and randomly as a PPP. *Lee & Haenggi* (2012) used Poisson cluster process to model the interference in a CRN. The bounds on the interference were derived in terms of a Laplace Transform to find the outage probability of the CRN. This paper assumed that a cognitive transmitter was active only when it was outside the PUs exclusion region.

Wen et al. (2010) analyzed the distribution of the AI in a CRN by considering the spatial PPP model and the average propagation path loss model. The outage, the throughput, and the ergodic capacity analysis were presented in *Haenggi* (2009) for a random wireless network. The ergodic rate calculations for multi-cell cellular networks using stochastic geometry were presented in *Andrews et al*. (2011). Apart from the network topology and the operational behavior, the type of channel fading is also important to decide the outage and the ergodic capacity of the network. *Nguyen & Sun* (2015) derived the upper and lower bounds of the signal to interference ratio (SIR) distribution under non-fading and Rayleigh fading conditions based on stochastic geometry. The ergodic capacity of the secondary link was derived for the Rayleigh fading channel with respect to the interference outage and signal to interference outage constraint in *Rezki & Alouini* (2012). Similar throughput analysis was carried out in *Song et al*. (2014) for the overlay CRN network by using opportunistic spectrum access. The path loss component estimation was carried out for the general fading channels including the Nakagami-m fading in *Srinivasa & Haenggi* (2009). The ergodic capacity analysis based on the moment generating function of the inverse of the SIR for multi-hop relaying channels in Nakagami-m fading was presented in *Triguiet al*. (2013). Previous works in the literature had studied the AI characterization at the P_{R_x} due to multiple SUs and had estimated the capacity of the CRN based on that aggregates the interference. The outage was calculated for the case when the SUs did not satisfy the threshold level of P_{R_x}. Most of the work presented in the literature assumes either no fading conditions or a Rayleigh fading model for the outage analysis.

This paper proposes the closed form equations for the outage probability of the secondary network based on the complementary cumulative distribution function (CCDF) of the received SIR at the SUs under the Nakagami-m fading channel. Further, the closed form expressions are derived for the ergodic capacity of the secondary network in Nakagami-m fading. The rest of the paper is organized as follows. Section 2 presents the system model based on the PPP. Section 3 explains the calculation of the Laplace Transform of AI. In section 4, the performance analysis is carried out to obtain the closed form equations for the outage probability and the ergodic capacity of the system. Section 5 presents the validation of the analytical results.

SYSTEM MODEL

The system model for aggregate interference characterization considers an Ad hoc and distributed network with nodes randomly placed in a finite Euclidean space. It is assumed here that all nodes are distributed as homogeneous spatial PPP. The CRN model has simplex primary systems in which the receivers are passive. It is mandatory for SUs to follow the interference avoidance laid by the regulators. Therefore, the protection margins required for P_{R_x} from SUs are mapped in terms of the distance. For better understanding of this paper, refer to Table 1 for the

important table of symbols used in this paper.

Table 1. Table of symbols.

Symbol	Meaning
λ	Intensity of interference sources in PPP
r	Spatial distance of the node
α	Path loss component
θ	SINR threshold level
m	Fading parameter of Nakagami fading
η	$2/\alpha$
Ω	Received average SNR

The characterization of AI in CRN is carried out by considering the spatial stochastic model as shown in Fig. 1.

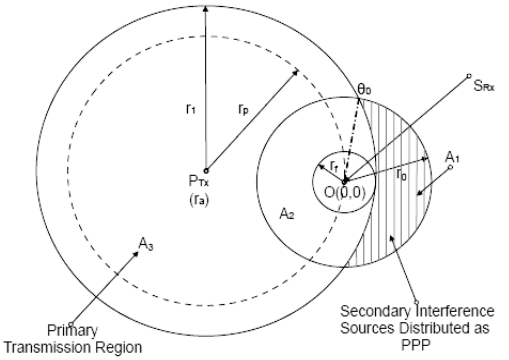

Figure 1. System model for cognitive radio Ad hoc. Network

A passive primary terrestrial TV network along with secondary TVWS network is considered here. The system model considers distributed network with nodes randomly spaced in a finite Euclidian space. The primary transmitter P_{T_x} is located at $r_a$and has a coverage region of radius r_1. The second dotted circle with radius r_p represents the maximum area covered by the primary network with minimum interference at the P_{R_x}. The coverage area of primary network is $A_p = A(r_a, r_1)$. Therefore, any P_{R_x}located beyond this region will undergo worst case interference. All secondary nodes are assumed to be distributed as homogeneous spatial PPP. The secondary receiver $S_{R_x}$is located at the centre or origin of PPP-$O(0,0)$. The forbidden region of the secondary system is shown by a circle with radius r_f. It is assumed that no secondary transmitter should transmit within this region as this region is referred to as the no-talk region of secondary receiver. P_{R_x} is assumed to be located at a distance of r_p from P_{T_x} so that it will have negligible interference from P_{T_x}. All other multiple SUs are assumed to be distributed spatially as PPP(ϕ) with intensity λ around the origin. The circle with radius r_0 represents the region that contributes the maximum AI at the secondary receiver. Therefore, it defines the interference region with area $\mathrm{A_I} = \mathcal{A}(0, \mathrm{r_f})/\mathcal{A}(0, \mathrm{r_0})$. The SUs, which are in the interference region, are only considered for the calculation of AI and outage analysis. The interference region is restricted within radius of $\mathrm{r_o}$. Here, the formation of physical structure of the nodes is not considered.

If we consider infinite network with $r_o \to \infty$, this gives

$$1 - {r_o}^{2-\alpha} > 1 - \epsilon \Rightarrow r_o > \epsilon^{-1/(\alpha-2)} \tag{1}$$

where α is path loss constant and ϵ denotes radius of ball around the origin. If $\epsilon = 0.1$ and $\alpha = 4$, then $r_o > 3.5$. This will consider the case of secondary network in rural area deployed over 3.5 Km radius used for secondary TV broadcasting networks. The AI at S_{R_x} and also at P_{R_x} is major due to other SUs in the interference region and very little due to P_{T_x} as it is on the protection radius. For the proposed system model, the following definitions are used.

Definition 1: The propagation model can be defined for power received by the primary and secondary receivers located at origin from P_{T_x} using isotropic path loss function as $l(r) = \|r\|^{-\alpha}$, where α is path loss function, which can be considered as $\leq \alpha \leq 4$ depending on the antenna height and terrain.

Definition 2: The AI at the receiver located at arbitrary distance z due to multiple secondary transmitters distributed as PPP (Φ) with intensity λ around origin $\mathcal{O}(0,0)$ is defined as

$$I(z) = \sum_{r \in \Phi} P_r \, h_r \, l(\|z - r\|) \tag{2}$$

where P_r is the interference power, h_r is the fading channel gain for interference, and $l(\|z - r\|) = \|r\|^{-\alpha}$ is a path loss function.

The average signal to interference noise ratio (SINR) at the receiver located at the origin of PPP is defined as

$$\text{SINR} = \frac{P_x g_x r^{-\alpha}}{\sigma^2 + \sum_{r \in \Phi} P_r \, h_r \|r\|^{-\alpha}} \tag{3}$$

where P_x is the received power at secondary receiver, g_x is the fading channel gain for signal, and σ^2 is the average noise power.

If the channel between σ^2 and S_{R_x} is Nakagami-m for fading, PDF of power fading coefficient $y = g_x$ is given by

$$p(y) = \frac{m^m}{\Omega^m \Gamma(m)} y^{m-1} e^{-\frac{my}{\Omega}} \tag{4}$$

where m describes the severity of fading for the desired link with $m = 1$ being a special case of Rayleigh fading and $m = \infty$ being no fading case and Ω– is the average SNR.

Let θ be the threshold level; the probability of outage in interference limited network is given by $P_o = 1 - P_s$, where P_s is the probability of correct reception. Here, P_s is also referred to as CCDF of SINR and denoted as $P_s = P[\text{SINR} > \theta]$.

To obtain the probability of outage, the CCDF of the received SINR is derived as

$$P[\text{SINR} > \theta] = P\left[\frac{P_x g_x r^{-\alpha}}{\sigma^2 + \sum_{r \in \Phi} P_r \, h_r \|r\|^{-\alpha}} > \theta\right]$$

$$P[\text{SINR} > \theta] = P\left[g_x > \left(\sigma^2 + \sum_{r \in \Phi} P_r \, h_r \|r\|^{-\alpha}\right) \frac{\theta r^{\alpha}}{P_x}\right] \tag{5}$$

$$P[\text{SINR} > \theta] = P\left[g_x > I \frac{\theta r^{\alpha}}{P_x}\right]$$

where $I = (\sigma^2 + \sum_{r\in\Phi} P_r\, h_r \|r\|^{-\alpha})$. By considering the interference power to be large compared to noise power as the number of interference sources contributes large interference power, they are close to the secondary receiver as given in *Deshmukh et al*. (2016).

$$I \approx \sum_{r\in\Phi} P_r\, h_r \|r\|^{-\alpha} \tag{6}$$

This gives

$$P[SINR > \theta] = \mathbb{E}\left(P\left[g_x > I\frac{\theta r^{\alpha}}{P_x}\right]\right) \tag{7}$$

Now, ,$P\left[g_x > I\frac{\theta r^{\alpha}}{P_x}\right] = \int_{I\frac{\theta r^{\alpha}}{P_x}}^{\infty} P(y)dy$ But $\Gamma(a,r) = \int_r^{\infty} t^{a-1}e^{-t}dt$,, This gives

$$P[SINR > \theta] = \mathbb{E}\left(P\left[g_x > P\left[g_x > I\frac{\theta r^{\alpha}}{P_x}\right] = \frac{-m^m(-1)^{m-1}}{(-m)^m}\left[\frac{\Gamma\left(m, \frac{m}{\Omega}\left(\frac{\theta r^{\alpha}}{P_x} I\right)\right]}{\Gamma(m)}\right] I\frac{\theta r^{\alpha}}{P_x}\right]\right) \tag{8}$$

But $\frac{\Gamma(m,my)}{\Gamma(m)} = e^{-my}\sum_{k=0}^{m-1}\frac{m^k}{k!}y^k$, where k is a positive integer. Equation (8) can be written as

$$P\left[g_x > I\frac{\theta r^{\alpha}}{P_x}\right] = e^{-\frac{m\theta r^{\alpha}}{\Omega P_x} I}\sum_{k=0}^{m-1}\frac{\left(\frac{\theta r^{\alpha}}{P_x}\frac{m}{\Omega}\right)^k}{k!} I^k \tag{9}$$

Putting Equation (9) into Equation (7),

$$P[SINR > \theta] = \mathbb{E}\left(e^{-\frac{m\theta r^{\alpha}}{\Omega P_x} I}\sum_{k=0}^{m-1}\frac{\left(\frac{\theta r^{\alpha}}{P_x}\frac{m}{\Omega}\right)^k}{k!} I^k\right) = \int_0^{\infty}\left(e^{-\frac{m\theta r^{\alpha}}{\Omega P_x} I}\sum_{k=0}^{m-1}\frac{\left(\frac{\theta r^{\alpha}}{P_x}\frac{m}{\Omega}\right)^k}{k!} I^k\right) f_i(i)di \tag{10}$$

where $f_i(i)$ is the PDF. Let $s = \frac{m}{\Omega}\frac{\theta r^{\alpha}}{P_x}$. Using the series expansion, the above equation can be written as

$$P[SINR > \theta] = \int_0^{\infty}\left(e^{-s\,I}\left[1 + s\,I + \frac{1}{2}(s^2I^2) + \cdots\right]\right) f_i(i)di \tag{11}$$

$$P[SINR > \theta] = \left(\left[s^0\int_0^{\infty} e^{-s\,I}I^0\, f_i(i)di\right] + \left[s^1\int_0^{\infty} e^{-s\,I}I^1\, f_i(i)di\right] + \frac{1}{2}\left[s^2\int_0^{\infty} e^{-s\,I}I^2\, f_i(i)di\right] + \cdots\right)$$

Using the property of Laplace transform as $x^n f(x) \overset{\mathcal{L}}{\Leftrightarrow} (-1)^n\frac{d^n\mathcal{L}_I(s)}{ds^n}$, Equation (11) can be written as

$$P[SINR > \theta] = \left[\sum_{k=0}^{m-1}\frac{s^k}{k!}(-1)^k\frac{d^k\mathcal{L}_I(s)}{ds^k}\right] \tag{12}$$

where $\mathcal{L}_I(s)$ is the Laplace transform of the AI at the secondary receiver. In order to derive the CCDF and probability of outage, it is necessary to first estimate the Laplace transform of aggregate interference.

CHARACTERIZATION OF AGGREGATE INTERFERENCE

The AI estimation is based on the PPP model explained in section 2 and as per the spatial distance model presented in Figure 1. The Laplace transform of AI at the receiver located at distance 'z' is given by

$$\mathcal{L}_I(s) \triangleq \mathbb{E}\left(e^{-s\,I(z)}\right) \tag{13}$$

where $I(z)$ is the AI at receiver defined in Equation (2).

$$\mathcal{L}_I(s)\big|_{s=\frac{m\theta r^{\alpha}}{\Omega\, P_X}} \triangleq \mathbb{E}\left(e^{-s\,\sum_{r\in\Phi} h_r \|r\|^{-\alpha}}\right) \tag{14}$$

The formulation of this AI is adapted from the calculations of interference for PPP in *Lee & Haenggi* (2012). Further, the Laplace transform of AI is calculated by considering probability generating functional (PGFL) with PPP defined by $S \subseteq \mathbb{R}^d$ as discussed in *Deshmukh et al*. (2016) as

$$\mathcal{L}_I(s) = \exp[-\lambda\,\pi\,\mathbb{E}(h_r{}^{\eta})\,\Gamma(1-\eta)s^{\eta}] \tag{15}$$

where $\eta = d/\alpha$ and for $\mathbb{R}^2$, $\eta = 2/\alpha$ and $\Gamma(.)$ represents Gamma Function.

In case of Rayleigh fading, $\mathbb{E}(h_r{}^{\eta}) = \Gamma(1+\eta)$ and for Nakagami-m fading channel

$$\mathbb{E}(h_r{}^{\eta}) = \frac{\Gamma(m+\eta)}{m^{\eta}\Gamma(m)} \quad \text{for } \eta \in \mathbb{R}^{+} \tag{16}$$

where m is the severity of fading, Therefore, Laplace transform of AI for Nakagami-m fading channel is given as

$$\mathcal{L}_I(s) = \exp\left[-\lambda\,\pi\,\frac{\Gamma(m+\eta)}{m^{\eta}\Gamma(m)}\quad \Gamma(1-\eta)s^{\eta}\right] \tag{17}$$

Further, to evaluate the outage performance, it is necessary to calculate the contribution of AI from region A_1, in Figure 1, at the origin of the process. Laplace transform of interference in the shaded region A_1 can be calculated by considering the limits of r from r_1 to r_0 and θ as the angle of intersection between the two regions from θ_0 to θ_1. Therefore, Equation (17) can be modified for AI in the shaded region of A_1 as given in *Deshmukh et al*. (2016).

$$\mathcal{L}_{I_o(A_1)}(s) = \exp[-\lambda\,\pi s^{\eta}\mathbb{E}(h_r{}^{\eta})2\theta_1[\Gamma(1-\eta,r_0) - \Gamma(1-\eta,r_1)]] \tag{18}$$

For Nakagami-m fading channel, this Laplace transform of AI in the shaded region of A_1 is

$$\mathcal{L}_{I_o(A_1)}(s) = \exp\left[-\lambda\,\pi s^{\eta}\frac{\Gamma(m+\eta)}{m^{\eta}\Gamma(m)}2\theta_1[\Gamma(1-\eta,r_0) - \Gamma(1-\eta,r_1)]\right] \tag{19}$$

If $\beta = 2\theta_1\lambda\,\pi[\Gamma(1-\eta,r_0) - \Gamma(1-\eta,r_1)]$,

$$\mathcal{L}_{I_o(A_1)}(s) = \exp\left[-\beta\, s^{\eta}\frac{\Gamma(m+\eta)}{m^{\eta}\Gamma(m)}\right] \tag{20}$$

By taking inverse Laplace transform of Equation (20), the PDF of the AI is obtained as

$$f_I(r) = \left[\frac{\beta_1 e^{-\frac{\beta_1{}^2}{4r}}}{2\sqrt{\pi}\, r^{3/2}}\right] \tag{21}$$

where $\beta_1 = 2\theta_1\lambda\,\pi[\Gamma(1-\eta,r_0) - \Gamma(1-\eta,r_1)\frac{\Gamma(m+\eta)}{m^{\eta}\Gamma(m)}$

PERFORMANCE ANALYSIS

The performance analysis of the secondary receiver for CRN is carried out by deriving closed form equations for outage probability and ergodic capacity under the Nakagami-m fading channel.

Outage probability analysis

The outage probability at the secondary receiver located at origin $\mathcal{O}(0,0)$ due to multiple secondary interference sources distributed as PPP and due to primary transmitter is derived by using Equations (12), (17), and (20). The analysis is carried out by considering the Nakagami-m fading channel.

Substituting Equation (20) into Equation (12), the CCDF of received SINR is obtained as

$$\mathrm{P}[\mathrm{SINR} > \theta] = \left[\sum_{k=0}^{m-1} \frac{s^k}{k!}(-1)^k \frac{d^k\left(\exp\left[-\beta\, s^{\eta}\frac{\Gamma(m+\eta)}{m^{\eta}\Gamma(m)}\right]\right)}{ds^k}\right] \tag{22}$$

The outage probability is given as $\mathrm{P_o} = 1 - \mathrm{P}[\mathrm{SINR} > \theta]$,

$$\mathrm{P_o} = 1 - \left[\sum_{k=0}^{m-1} \frac{s^k}{k!}(-1)^k \frac{d^k\left(\exp\left[-\beta\, s^{\eta}\frac{\Gamma(m+\eta)}{m^{\eta}\Gamma(m)}\right]\right)}{ds^k}\right] \tag{23}$$

The probability of outage over the complete plane is derived as

$$\overline{\mathrm{P}}_o = 1 - \int_o^{\infty} \mathrm{P}[\mathrm{SINR} > \theta] f_r(r)\, dr \tag{24}$$

where $f_r(r)$ is PDF of r given by *Andrews et al*. (2011) as $f_r(r) = e^{-\lambda\pi r^2} 2\pi\lambda r$,

$$\overline{\mathrm{P}}_o = 1 - \int_o^{\infty} \left[\sum_{k=0}^{m-1} \frac{s^k}{k!}(-1)^k \frac{d^k\left(\exp\left[-\beta\, s^{\eta}\frac{\Gamma(m+\eta)}{m^{\eta}\Gamma(m)}\right]\right)}{ds^k}\right] e^{-\lambda\pi r^2} 2\pi\lambda r\ dr \tag{25}$$

The closed form expression of this outage probability is obtained for three different cases of m being the fading parameter for Nakagami-m fading channel.

Case I: $m = 1$ and $\alpha = 4$,

$$\overline{\mathrm{P}}_o = 1 - \int_o^{\infty} \left[e^{-0.886\beta\sqrt{s}}\right] e^{-\lambda\pi r^2} 2\pi\lambda r\, dr$$

But $s = \frac{m}{\Omega}\frac{\theta r^{\alpha}}{P_x}$,

$$\overline{\mathrm{P}}_o = 1 - \frac{\lambda\pi}{0.886\,\beta\sqrt{\frac{\theta}{\Omega P_x}} + \lambda\pi} \tag{26}$$

Case II: $m = 2$ and $\alpha = 4$,

$$\overline{\mathrm{P}}_o = 1 - \int_o^{\infty} \left[e^{-\beta x^2} - 0.47\beta\sqrt{s}e^{-0.94\beta\sqrt{s}}\right] e^{-\lambda\pi r^2} 2\pi\lambda r\, dr$$

But, $s = \frac{m}{\Omega}\frac{\theta r^{\alpha}}{P_x}$

$$\overline{\mathrm{P}}_o = 1 - \frac{\lambda\pi}{\left(0.94\beta\sqrt{\frac{2\theta}{\Omega P_x}} + \lambda\pi\right)^2} \tag{27}$$

Case III: $m = 3$ and $\alpha = 4$,

$$\overline{P}_o = 1 - \int_o^{\infty} \left[e^{-0.96\beta\sqrt{s}} + s\frac{d\left(e^{-0.96\beta\sqrt{s}}\right)}{ds} + \frac{s^2}{2}\frac{d^2\left(e^{-0.96\beta\sqrt{s}}\right)}{ds^2} \right] e^{-\lambda\pi r^2} 2\pi\lambda r \, dr$$

But, $s = \frac{m}{\Omega}\frac{\theta r^{\alpha}}{P_x}$

$$\overline{P}_o = 1 - \left[\frac{25\lambda\pi}{24\,B + 25\lambda\pi} + \frac{\lambda\pi B}{(2B + \lambda\pi)^2} + \frac{25\lambda\pi B}{2(100B + \lambda\pi)^2} + \frac{2500\lambda\pi B^2}{(100B + \lambda\pi)^3} \right] \quad (28)$$

where $B = 0.0096\beta\sqrt{\frac{\theta}{\Omega P_x}}$

Ergodic capacity analysis

The ergodic capacity of the secondary system by considering the multiple secondary interference sources distributed as PPP is derived by taking the average over both the spatial PPP and fading distribution. Fading distribution is assumed to be Nakagami-m fading.

The ergodic capacity is $C_E \triangleq \mathbb{E}(\ln(1 + SINR))$. From Equation (3),

$$C_E \triangleq \int_{r>0} e^{-\lambda\pi r^2} \mathbb{E}\left(\ln\left(1 + \frac{P_x g_x r^{-\alpha}}{\sigma^2 + \sum_{r\in\Phi} P_r\, h_r \|r\|^{-\alpha}}\right)\right) 2\pi\lambda r \; dr \quad (29)$$

$$C_E = \int_{r>0} \left[\int_{\theta>0} \mathbb{P}\left(\ln\left(1 + \frac{P_x g_x r^{-\alpha}}{\sigma^2 + \sum_{r\in\Phi} P_r\, h_r \|r\|^{-\alpha}}\right) > \theta \right) d\theta \right] e^{-\lambda\pi r^2} 2\pi\lambda r \; dr \quad (30)$$

As $I_r = \sum_{r\in\Phi} P_r\, h_r \|r\|^{-\alpha}$

$$C_E = \int_{r>0} \left[\int_{\theta>0} \mathbb{P}\left(g_x > (e^{\theta} - 1)\, \frac{(\sigma^2 + I_r)\, r^{\alpha}}{P_x} \right) d\theta \right] e^{-\lambda\pi r^2} 2\pi\lambda r \, dr \quad (31)$$

If the noise power is assumed to be $(\sigma^2 = 1)$,

$$C_E = \int_{r>0} \left[\int_{\theta>0} \underbrace{\mathbb{P}\left(g_x > (e^{\theta} - 1)\, \frac{I_r r^{\alpha}}{P_x} \right)}_{T_3} d\theta \right] e^{-\lambda\pi r^2} 2\pi\lambda r \, dr \quad (32)$$

Further, T_3 is solved by using the method of Equation (9)

$$T_3 = \mathbb{P}\left(g_x > (e^{\theta} - 1)\, \frac{I_r r^{\alpha}}{P_x} \right) = \int_{(e^{\theta}-1)\frac{I_r r^{\alpha}}{P_x}}^{\infty} p(y)\, dy \quad (33)$$

But, $\Gamma(a, x) = \int_x^{\infty} t^{a-1} e^{-t} dt = \frac{-m\,(-1)^{m-1}}{(-m)^m} \left[\frac{\Gamma\left(m, \frac{m(e^{\theta}-1) r^{\alpha}}{\Omega\ P_x} I_r \right)}{\Gamma(m)} \right]$ and

$\Gamma(m, m_y) = e^{-m_y} \sum_{k=0}^{m-1} \frac{m^k}{k!} y^k$, Therefore,

$$T_3 = \mathbb{E}\left(e^{-\frac{m(e^{\theta}-1) r^{\alpha}}{\Omega\ P_x} I_r} \sum_{k=0}^{m-1} \frac{\left(\frac{(e^{\theta}-1) r^{\alpha}}{P_x} \frac{m}{\Omega} \right)^k}{k!} {I_r}^k \right) \quad (34)$$

By using the method of Equation (12),

$$T_3 = \sum_{k=0}^{m-1} \frac{s^k}{k!} (-1)^k \frac{d^k \mathcal{L}_I(s)}{ds^k} \qquad \text{where,} \qquad s = \frac{m}{\Omega} \frac{(e^{\theta} - 1) r^{\alpha}}{P_x} \quad (35)$$

Substituting Equation (35) into Equation (32)

$$C_E = \int_{r>0}\left[\int_{\theta>0}\sum_{k=0}^{m-1}\frac{s^k}{k!}(-1)^k\frac{d^k\mathcal{L}_I(s)}{ds^k}d\theta\right]e^{-\lambda\pi r^2}2\pi\lambda r\,dr \tag{36}$$

where from Equation (20), $\mathcal{L}_I(s) = \exp\left[-\beta\, s^\eta \frac{\Gamma(m+\eta)}{m^\eta\Gamma(m)}\right]$

Further, the closed form expressions for the ergodic capacity are obtained for the three different cases of 'm', being fading parameter of Nakagami-m fading channel.

Case I: $m = 1$ and $\alpha = 4$,

$$C_E = \int\limits_{r>0}\left[\int\limits_{\theta>0} e^{-0.886\beta\sqrt{s}}d\theta\right]e^{-\lambda\pi r^2}2\pi\lambda r\,dr \tag{37}$$

where $\beta = 2\theta_1\lambda\,\pi[\Gamma(1-\eta, r_0) - \Gamma(1-\eta, r_1)]$

Interchanging the integration sequence and by using $s = \frac{m}{\Omega}\frac{(e^\theta-1)r^\alpha}{P_x}$,

$$\begin{gathered} C_E = \int\limits_{\theta>0}\left[\int\limits_{r>0} e^{-0.886\beta\sqrt{\frac{(e^\theta-1)}{\Omega P_x}}r^2} e^{-\lambda\pi r^2}2\pi\lambda r\,dr\right]d\theta \\ C_E = \int\limits_{\theta>0}\frac{\pi\lambda}{\pi\lambda + 0.886\beta\sqrt{\frac{(e^\theta-1)}{\Omega P_x}}}d\theta = \int\limits_{\theta>0}\left[\frac{\pi\lambda}{\pi\lambda + \beta_1\sqrt{(e^\theta-1)}}\right]d\theta \end{gathered} \tag{38}$$

where $\beta_1 = \frac{0.886\beta}{\sqrt{\Omega P_x}}$

$$\begin{aligned} C_E = \frac{\pi\lambda}{\pi^2\lambda^2 + {\beta_1}^2}\Bigg[&-\pi\lambda\log\left(\pi^2\lambda^2 - {\beta_1}^2 e^\theta + {\beta_1}^2\right) - 2\pi\lambda\tanh^{-1}\left(\frac{\beta_1\sqrt{(e^\theta-1)}}{\pi\lambda}\right) + \pi\lambda\theta \\ &+ 2\beta_1\tan^{-1}\left(\sqrt{(e^\theta-1)}\right)\Bigg] \end{aligned} \tag{39}$$

Case II: $m = 2$ and $\alpha = 4$,

$$C_E = \int\limits_{r>0}\left[\int\limits_{\theta>0} e^{-\beta r^2} + s\,\frac{de^{-0.94\beta s^\eta}}{ds}\;d\theta\right]e^{-\lambda\pi r^2}2\pi\lambda r\,dr \tag{40}$$

Similar to Case I approach, by interchanging and solving the inner integral

$$C_E = \int\limits_{\theta>0}\frac{\pi\lambda}{\left(\pi\lambda + 0.94\beta\sqrt{\frac{2(e^\theta-1)}{\Omega P_x}}\right)^2}d\theta = \int\limits_{\theta>0}\left[\frac{\pi\lambda}{\left(\pi\lambda + 2\beta_2\sqrt{(e^\theta-1)}\right)^2}\right]d\theta \tag{41}$$

where $\beta_2 = 0.47\beta\sqrt{\frac{2}{\Omega P_x}}$. Solving the integral

$$\begin{aligned} C_E = \frac{\pi\lambda}{\left(\pi^2\lambda^2 + 4{\beta_2}^2\right)^2}\Bigg[&\frac{\left(\pi^2\lambda^2 + 4{\beta_2}^2\right)(2\pi^2\lambda^2 - 4\pi\lambda\beta_2\sqrt{(e^\theta-1)})}{B_2} + \theta B_1 - B_1\log(B_2) \\ &- 2B_1\tanh^{-1}\left(\frac{2\beta_2\sqrt{(e^\theta-1)}}{\pi\lambda}\right) + 8\pi\lambda\,\beta_2\tan^{-1}(\sqrt{(e^\theta-1)})\Bigg] \end{aligned} \tag{42}$$

where $B_1 = \left(\pi^2\lambda^2 - 4{\beta_2}^2\right)$ and $B_2 = \pi^2\lambda^2 - 4{\beta_2}^2(e^{\theta} - 1)$

Case III: $m = 3$ and $\alpha = 4$,

$$C_E = \int_{r>0}\left[\int_{\theta>0} e^{-0.96\beta\sqrt{s}} + s\,\frac{d\left(e^{-0.96\beta\sqrt{s}}\right)}{ds} + s^2\frac{d^2\left(e^{-0.96\beta\sqrt{s}}\right)}{ds^2}d\theta\right]e^{-\lambda\pi r^2}2\pi\lambda r\,dr \tag{43}$$

$$C_E = \int_{\theta>0}\left[\frac{25\pi\lambda}{25\pi\lambda + 24B_3} + \frac{\pi\lambda B_3}{(\pi\lambda + 2B_3)^2} + \frac{25\pi\lambda B_3}{2(\pi\lambda + 100B_3)^2} + \frac{2500\pi\lambda {B_3}^2}{(\pi\lambda + 100B_3)^3}\right]d\theta \tag{44}$$

where $B_3 = \frac{0.0096\beta}{\sqrt{\Omega P_x}}\sqrt{(e^{\theta} - 1)}$.

Integrations of Equation (44) are solved by using the integrator solver like wolfram or Symbolab. The results are verified for this equation for various parameters in the Results and Discussions section.

RESULTS AND DISCUSSIONS

To characterize the performance measure, the outage probability and ergodic capacity are considered as quality of service (QoS) metric for CRN. All CRN users have to work under strict interference constraints of the primary network. Therefore, the estimation of AI at the primary and secondary receiver due to primary transmitter and multiple CRN nodes distributed as PPP is carried out in section 3. Here, the Laplace transform of this AI and its PDF are derived at origin of PPP. The PDF of this AI depends on the spatial distance r and the intensity λ of PPP as shown in Figure 2.

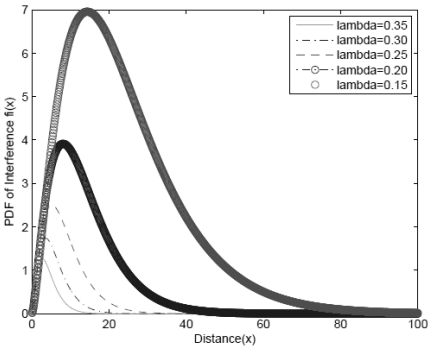

Figure 2. PDF of the aggregate interference at the origin of PPP.

Outage probability derived in section 4 is affected by many parameters such as spatial distance, intensity of PPP, threshold level, and the fading parameters. Outage probability is an increasing function of SINR threshold as shown in Figure 3. The comparison of three cases derived in section 4 for different values of fading parameters is shown here. Case I, with $m = 1$ and $\alpha = 4$, describes the special case of Nakagami-m fading channel approximated as Rayleigh fading. It shows maximum outage and should be operated at very small SINR threshold levels. As m increases further, the outage probability decreases and the higher values of SINR threshold can be selected, this will increase the secondary link performance.

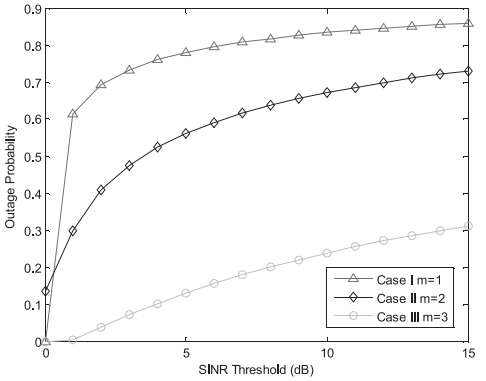

Figure 3. Outage probability of secondary CRN for different values of 'm' with $\lambda = 0.35$ and $\alpha = 4$.

In designing the network topology, it is highly important to consider the intensity and the distribution of nodes. The AI also depends on the intensity of PPP; therefore, the outage probability will also vary depending upon the values of λ. Figure 4 shows the outage probability for different values of λ. It is observed that as λ decreases, the outage will go on increasing. Ergodic capacity is another important parameter that ensures the QoS of CRN.

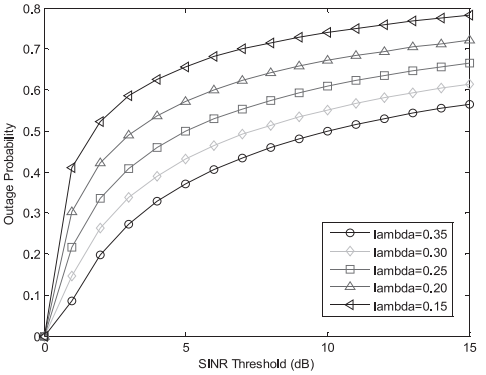

Figure 4. Outage probability of secondary CRN for different values of λ with m=1, $\alpha = 4$.

In Section 5, the closed form equations are derived for ergodic capacity of secondary network under Nakagami-m fading channel. The capacity of system also depends on various parameters such as SINR threshold level, fading parameter, intensity of PPP, and average received SNR.

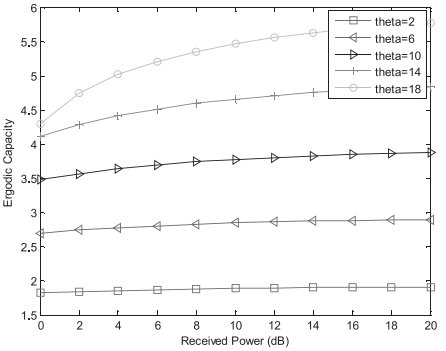

Figure 5. Ergodic capacity of secondary CRN under average receiver power for different values of SINR threshold.

In order to validate the derived equations, the impact of all these parameters on ergodic capacity

is verified by simulations. Figure 5 shows ergodic capacity of secondary link under average received power for different values of SINR threshold. As threshold increases, the received signal strength of the signal increases. This will help increase the ergodic capacity of the system.

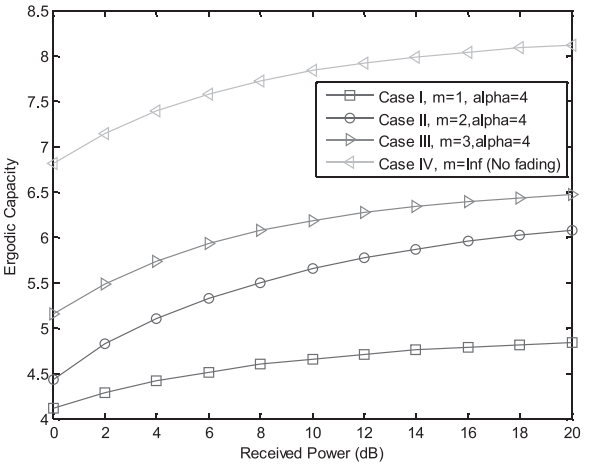

Figure 6. Ergodic capacity of secondary CRN under average receiver power for different values of 'm' with $\lambda = 0.35$ and $\alpha = 4$.

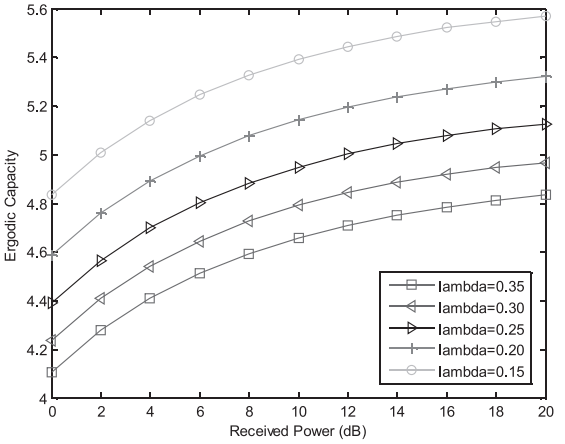

Figure 7. Ergodic capacity of secondary CRN under average receiver power for different values of 'λ' with $m = 1$ and $\alpha = 4$.

The ergodic capacity for different values of fading parameters for Nakagami-m fading is shown in Figure 6. Here, the ergodic capacity increases with value of 'm' and gives less capacity with m=1 for the Rayleigh fading case. Figure 7 shows the variation with respect to intensity λ of PPP. The ergodic capacity increases with the decrease in intensity λ. The closed formed expressions are also verified with variation in the received average SNR (Ω) values in Figure 8. Here, ergodic capacity increases along with the values of Ω.

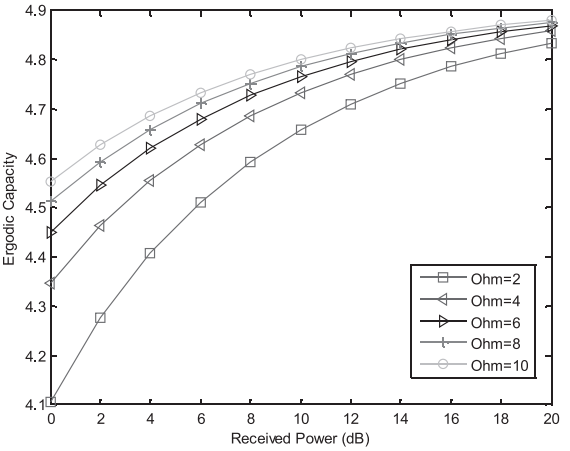

Figure 8. Ergodic capacity of secondary CRN under average receiver power for different values of 'Ω' with $m = 1, \lambda = 0.35$ and $\alpha = 4$.

CONCLUSION

In this paper, the characterization of AI at both primary and secondary receivers is carried out due to multiple secondary receivers. The system model is designed by using stochastic geometry tools where all interfering nodes are assumed to be distributed as PPP. The result shows that the interference at the primary receiver located at a protection radius r_p and arbitrarily located secondary receiver is largely contributed by the secondary transmitters outside the protection radius under imperfect sensing conditions. Further, the closed form equations are derived for the outage probability under Nakagami-m fading for different fading conditions. The analytical results are validated for different parameters such as spatial distance, intensity of PPP, threshold level, and the fading parameters. In addition, exact closed form expressions were obtained for ergodic capacity of secondary link under the impact of AI due to a primary transmitter and multiple secondary transmitters. The results show that the outage probability and ergodic capacity depend on not only the threshold levels of primary receiver, but also a function of received SINR at secondary receiver, network topology, and the fading parameters of Nakagami-m fading. Further the formulation of the outage and ergodic capacity of secondary CRN can be used in selecting the subset of antenna in multiple antenna systems deployed for secondary transmitter in CRN.

REFERENCES

Ahmad A., Hakim G., Elias Y., Alouini M. & Kamal A., 2015. Joint Bandwidth and Power Allocation for MIMO Two-Way Relays-Assisted Overlay Cognitive Radio Systems. IEEE Transactions on Cognitive Communications and Networking. 1 (4):383-393.

Andrews, J., Bacceel, F. & Ganti, R. K., 2011. A Tractable Approach to Coverage and Rate in Cellular Networks. IEEE Transactions on Communications, 59(11): 3122-3134.

Baccelli, F. & Blaszczyszyn, B., 2009. Stochastic Geometry and Wireless Networks.Vol-II-Applications. B. NoW Publishers.

Chen, Z., Wang, C., Hong, X. & Thompson, J., 2012. Aggregate Interference Modeling in Cognitive Radio Networks with Power and Contention Control. IEEE Transactions on Communications, 60(2): 456-468

Deshmukh, M., Mihvoska A., Federiksen, F. B. & Prasad, R., 2016. . Interference Characterization in TVWS based CRNs: A spatial statistical approach.(Unpublished data)

Goldsmith, A. & Maric, I., 2013. Capacity of Cognitive Radio Networks. In: Principles of Cognitive Radio. Pp. 1-66. Cambridge University Press.

Haenggi, M. & Ganti, R. K., 2009. . Interference in Large Wireless Networks. Foundations and Trends in Networking,, 3(2): 127-248.

Haenggi, M., 2009. Outage, Local Throughput, and Capacity of Random Wireless Networks. IEEE Transactions on Wireless Communications, 8(8): 4350-4359.

Haenggi, M., Andrews, J. & Baccelli, F., 2009. Stochastic Geometry and Random Graphs for the Analysis and Design of Wireless Networks. IEEE Journal on selected areas in communications, 27(7): 1029-1046

Jabbari, B. & Babaei, A., 2008. Internodal Distance Distribution and Power Control for Coexisting Radio Networks. In IEEE Global Telecommunications Conference. New Orleans, LO,1-5.

Lee, C. & Haenggi, M., 2012. Interference and Outage in Poisson Cognitive Networks. IEEE Transactions on Wireless Communications, 1(4): 1392-1401.

Mitola, J. & Maquire, G.Q., 1999. Cognitive Radio: Making Software Radios more Personal. IEEE Personal Communicatios, 6(4):13-18.

Nguyen, H. & Sun, S, 2015. Stochastic Geometry-based Performance Bounds for Non-Fading and Rayleigh Fading Ad-hoc Networks. [Online]. Available at: arXiv:1509.04002.

Rezki, Z. & Alouini, M. S., 2012. Ergodic Capacity of Cognitive Radio under Imperfect Channel State Information. IEEE Transactions on Vehicular Technology, 61(5): 2108-2119.

Song, X., Yin, C., Liu, D. & Zhang, R., 2014. Spatial Throughput Characterization in Cognitive Radio Networks with Threshold-based Opportunistic Spectrum Access. IEEE Journal on Selected Areas in Communications, 32(11): 2190.2204.

Srinivasa, S. & Haenggi, M.,2009. Path loss exponent estimation in large wireless networks. In IEEE Information Theory and Applications Workshop. San Diego, CA, 124-129.

Srinivasa, S. & Haenggi, M, 2007. Modling Interfernce in Finite Uniformly Random Networks. In International Workshop on Information Theory for Sensor Networks. Santa Fe, NM, 1-7.

Timmers, M., Pollin, S., Dejonghe, A. & Bahai, A., 2008. Accumulative Interference Modeling for Cognitive Radios with Distributed Channel Access. In International Conference on Cognitive Radio Oriented Wireless Networks and Communications. Singapore, 1-7.

Trigui, I., Affes, S. & Stephenne, A., 2013. Ergodic Capacity Analysis for Interference-Limited AF Multi-Hop Relaying Channels in Nakagami-m Fading. IEEE Transactions on Communications, 61(7): 2726-2734.

Wen, Y., Loyka, S. & Yongacoglu, A.,2010. On distribution of aggregate interference in cognitive radio networks. In 25th Biennial Symposium on Communications (QBSC). Kingston, ON, 265-268.

Yang, Y., Hou, J. & Kung, L., 2007. Modeling the Effect of Transmit Power and Physical Carrier Sense in Multi-hop Wireless Networks. In 26th IEEE International Conference on Computer Communications, Institute of Electrrical and Elecronics Engineers(IEEE). Anchorage,AK, 2331-2335.

Weifeng S., Matyjas J. & Batalama S., 2012. Modeling the Effect of Transmit Power and Physical Carrier Sense in Multi-hop Wireless Networks. Active cooperation between primary users andcognitive radio users inheterogeneous Ad-Hoc networks. IEEE Transactions on Signal Processing, 60(4): 1796-1805.

Submitted: 12/06/2016
Revised : 03/12/2017
Accepted : 21/03/2017